Bull Math Biol (2014) 76:1194–1217
DOI 10.1007/s11538-014-9961-7

Society for Mathematical Biology

ORIGINAL ARTICLE

The Dynamics of Growing Islets and Transmission of *Schistosomiasis Japonica* in the Yangtze River

Chunhua Shan · Xiaonong Zhou · Huaiping Zhu

Received: 1 October 2012 / Accepted: 9 April 2014 / Published online: 24 April 2014

Abstract We formulate and analyze a system of ordinary differential equations for the transmission of *schistosomiasis japonica* on the islets in the Yangtze River, China. The impact of growing islets on the spread of schistosomiasis is investigated by the bifurcation analysis. Using the projection technique developed by Hassard, Kazarinoff and Wan, the normal form of the cusp bifurcation of codimension 2 is derived to overcome the technical difficulties in studying the existence, stability, and bifurcation of the multiple endemic equilibria in high-dimensional phase space. We show that the model can also undergo transcritical bifurcations, saddle-node bifurcations, a pitchfork bifurcation, and Hopf bifurcations. The bifurcation diagrams and epidemiological interpretations are given. We conclude that when the islet reaches a critical size, the transmission cycle of the *schistosomiasis japonica* between wild rats *Rattus norvegicus* and snails *Oncomelania hupensis* could be established, which serves as a possible source of schistosomiasis transmission along the Yangtze River.

Keywords Schistosomiasis · Growing islet · Transmission dynamics · Cusp bifurcation of codimension 2 · Transcritical bifurcation · Saddle-node bifurcation · Pitchfork bifurcation · Hopf bifurcation

1 Introduction

Schistosomiasis is a parasitic disease affecting at least 240 million people worldwide, and more than 700 million people living in endemic areas are at risk

C. Shan · H. Zhu (✉)
Department of Mathematics and Statistics, York University, Toronto, ON M3J 1P3, Canada
e-mail: huaiping@mathstat.yorku.ca

X. Zhou
National Institute of Parasitic Disease, Chinese Center for Disease Control and Prevention, Shanghai, China

(http://www.who.int/mediacentre/factsheets/fs115/en/index.html). It remains formidable to humans because of the complexities of parasitic adaptation to two or more different hosts. The persistence of this disease in a locality depends on a complex cycle of events involving humans or mammals (the definitive host), certain parasitic flatworms (the schistosome), and particular species of snails (the intermediate host). In this cycle, humans or mammals will become infected when they contact water containing the cercariae released from the infected snails, while snails will become infected when they are invaded by miracidia hatched from eggs, which are released by infected humans or other mammals (Anderson and May 1991; Gryseels et al. 2006).

The prevalence of *Schistosomiasis japonica* in China can trace back to thousands of years ago by the traditional records. The control program of schistosomiasis in China, launched in the 1950s and sustained over the past 60 years, is widely acknowledged as one of the most successful disease control programs (Zhou et al. 2005). However, the surveillance data suggest that schistosomiasis transmission has re-emerged in 38 counties from 7 provinces along the Yangtze River since the late 1990s, as both snail habitats and local transmission had been observed (Zhao et al. 2005; Zhou et al. 2002, 2005). The disease control is still a great challenge in endemic regions due to climate and environmental changes. Understanding the impact of these factors on the disease transmission is essential to the development of comprehensive control strategies.

In order to understand the mechanism between environmental changes and the schistosomiasis disease, we assess the patterns of the schistosomiasis transmission re-emerging in Qian islet and Zimu islet, two typical ones among the hundreds of islets in the Yangtze River, China (Fig. 1). Because of the sedimentation, two islets started to emerge from the water surface in 1970 and 1976, respectively. The areas of two islets have been expanding since their formulation (Xu et al. 1999). As of 2011, the area of Qian islet is 3.33 million m^2, and the area of Zimu islet is 5 million m^2.

The snails were discovered on Qian islet in 1980, 10 years after its emergence from the river, and the record showed that snails appeared on Zimu islet in 1984. The investigation carried out by the researchers from Nanjing Institute of Parasitic Diseases in the period of 1996–1998 indicated that schistosomiasis disease had presented in the two islets, and concluded that rats *Rattus norvegicus* were the primary definitive

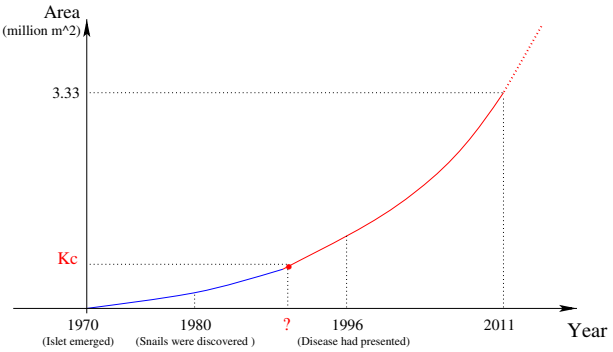

Fig. 1 Schematic diagram of the history of the schistosomiasis disease in Qian islet (Color figure online)

hosts and snails *Oncomelania hupensis* were the intermediate hosts of *Schistosoma japonicum* (Xu et al. 1999). From the land size evolution of the islets and outbreak of schistosomiasis, it is reasonable to connect the transmission of schistosomiasis with the growing sizes of the islets. In this paper, we will use mathematical models to explore the impact of the expansion of islets on the disease transmission and try to explain the re-emergence mechanism of *S. japonica* along the Yangtze River from the late 1990s.

There have been lots of mathematical studies of schistosomiasis since 1960s (Castillo-Chavez et al. 2008; Feng et al. 2002, 2005; Liang et al. 2002, 2007; MacDonald 1965; Nåsell and Hirsch 1973; Wu et al. 1987; Wu and Feng 2002; Zhang et al. 2007; Zhao and Milner 2008), etc. The first mathematical model of schistosomiasis was proposed and studied by MacDonald (1965), which is dated back to 1965. Since then much has been done in terms of modeling and analyses of transmission dynamics of schistosomiasis. Nåsell and Hirsch (1973) proposed a stochastic version of MacDonald's model. Wu et al. (1987) built and analyzed a schistosomiasis model, and then it was generalized with the multiple definitive hosts (Wu and Feng 2002). Mathematical models with mass chemotherapy in human hosts were formulated and studied by Feng et al. (2002). The schistosomiasis models with multigroups or age structure for human hosts were studied in Feng et al. (2005), Liang et al. (2002), Liang et al. (2007), Zhang et al. (2007). The delay during the schistosomiasis transmission was considered in Castillo-Chavez et al. (2008), Wu and Feng (2002). However, most of these models have ignored the impact of the environment, especially the natural carrying capacity for both the definitive hosts and the intermediate hosts, on the transmission of this disease.

For a finite or infinite dimensional dynamical system, the center manifold theorem plays an important role, which reduces the system to a lower dimension to make the analysis easier (Carr 1981). There are no theoretical difficulties in center manifold calculation. However, the calculation is rather complicated for a high or infinite dimensional system, and that is the reason why the bifurcation analyses of high codimension were carried out in the planar system in most papers. With the adjoint operator theory and the spectral decomposition, the projection technique developed in Hassard et al. (1981) to study the Hopf bifurcation in infinite dimensional system is very powerful for the center manifold calculation. In this paper, we will apply the projection technique to the bifurcation analysis due to the high dimension of our model.

The paper is organized as follows. In Sect. 2, we formulate a system of ordinary differential equations incorporating the impact of growing islets to model the mouse–snail cycle of schistosomiasis. This high-dimensional model can exhibit multiple endemic equilibria which results in complexity of dynamics and technical difficulties in studying the existence and stability of endemic equilibria. Therefore, in Sect. 3, we calculate the center manifold and normal form of the cusp bifurcation of codimension 2 to overcome these difficulties, and then study the Hopf bifurcation. The effect of the islet expansion on the disease transmission is obtained from the bifurcation analysis. In Sect. 4, numerical simulations are carried out to supplement and illustrate the theoretical results. The conclusion and control strategies are given in Sect. 5.

2 Formulation of the Model

According to the investigations by the researchers from Nanjing Institute of Parasitic Diseases (Xu et al. 1999), there are no human residents, livestock, or wild animals on Qian and Zimu islets. The rats *R. norvegicus* are the only definitive hosts, and the snails *O. hupensis* serve as the intermediate hosts. The ecosystem on these two islets is so ideal for our modeling, and we study the schistosomiasis transmission on any one of these two islets.

Suppose M_s and M_i are the numbers of susceptible and infected mice, respectively. Let S_s and S_i represent the numbers of susceptible and infected snails, respectively.

The growth of host population will be limited by intraspecific competitions for finite resources, so we assume that the populations of mice and snails on the islet follow the logistic growth. For the snails, more than 97 % of the infected female snails lose the reproduction ability because of the lesions and atrophy of gonads (Zhou 2005). There are few literatures concerning the impact of the disease on the reproduction ability of mammals. However, some researches have shown that schistosomiasis can damage the genital system of human beings, and results in ectopic pregnancy, infertility, abortion, increased infant mortality rate, cervical lesions, and cervical cancer (Poggensee and Feldmeier 2001; Poggensee et al. 1999), (http://www.who.int/mediacentre/factsheets/fs115/en/index.html). Therefore, we suppose that the infected snails and mice cannot reproduce, and the growth of the populations of the snails and mice is contributed by the susceptible classes.

According to the life cycle of schistosomiasis transmission, we know that the definitive hosts and intermediate hosts can infect each other via the cercariae and miracidia (Anderson and May 1991; Gryseels et al. 2006), and we assume that the cross-infection between mice and snails is subject to the mass action principle. Therefore, we formulate the schistosomiasis model involving the two hosts as follows:

$$\begin{cases} \dot{M}_s = r_m M_s \left(1 - \dfrac{M_s + \delta_1 M_i}{K_m}\right) - d_m M_s - \beta_m M_s S_i, \\ \dot{M}_i = \beta_m M_s S_i - (d_m + \mu_m) M_i, \\ \dot{S}_s = r_s S_s \left(1 - \dfrac{S_s + \delta_2 S_i}{K_s}\right) - d_s S_s - \beta_s M_i S_s, \\ \dot{S}_i = \beta_s M_i S_s - (d_s + \mu_s) S_i. \end{cases} \tag{1}$$

Here, r_m and r_s are the intrinsic growth rates of mice and snails, respectively. β_m and β_s are the transmission rates from the infected snails to susceptible mice and from the infected mice to susceptible snails, respectively. d_m and d_s denote the per capita nature death rates of mice and snails, and μ_m and μ_s are the per capita death rates of mice and snails induced by infection, respectively.

In model (1), K_m and K_s in the logistic growth terms are the spatial environmental capacities of the islet, which correspond to the maximum populations of mice and snails, respectively. Since the spatial environmental capacity depends on the physical size of the islet, if we let K (m^2) be the physical size of the islet, and denote the maximum densities of mice and snails per m^2 as k_m and k_s, then we can write $K_m = k_m K$ and $K_s = k_s K$.

It is apparent that the infected mice and snails do not share the same resources on the islet, so we introduce two positive parameters δ_1 and δ_2 in model (1) to measure the competition abilities between infected and susceptible classes of mice and snails, respectively.

For the infected snails, their digestive system especially the digestive gland is destroyed, and some organs loss their functions due to the connective tissue hyperplasia (Zhou 2005). For the infected mammals, the disease can induce the impaired physical and cognitive development. Severely infected animals deteriorate rapidly and usually die within a few months of infection, while those less heavily infected ones will develop chronic disease with the growth retardation.

Therefore, it is reasonable to presume that for the infected mice and snails, they have no enough energy and mobility to compete with the susceptible species for the sustaining resources, and we have $0 \le \delta_1 \ll 1, 0 \le \delta_2 \ll 1$. In the following analysis, we will consider a simplified version of model (1) by assuming that $\delta_1 = 0$ and $\delta_2 = 0$ and study the corresponding simplified model, and we have the following proposition.

Proposition 2.1 *For system* (1), $\overline{R^{4+}}$ *is invariant, and the solution exists globally.*

Proof First, the smoothness of functions at the right-hand side of system (1) insures the local existence and uniqueness of the system with the initial condition.

Second, $\dot{M}_{\mathrm{s}|M_{\mathrm{s}}=0} = 0, \dot{M}_{i\,|M_i=0} = \beta_{\mathrm{m}} M_{\mathrm{s}} S_i > 0, \dot{S}_{\mathrm{s}|S_{\mathrm{s}}=0} = 0, \dot{S}_{i\,|S_i=0} = \beta_{\mathrm{s}} M_i S_{\mathrm{s}} > 0$, so the solution with the initial value in $\overline{R^{4+}}$ will remain nonnegative for all $t \ge 0$.

From (1), we have

$$\dot{M}_{\mathrm{s}} \le r_{\mathrm{m}} M_{\mathrm{s}} \left(1 - \frac{M_{\mathrm{s}}}{K_{\mathrm{m}}}\right) - d_{\mathrm{m}} M_{\mathrm{s}} \quad \text{and} \quad \dot{S}_{\mathrm{s}} \le r_{\mathrm{s}} S_{\mathrm{s}} \left(1 - \frac{S_{\mathrm{s}}}{K_{\mathrm{s}}}\right) - d_{\mathrm{s}} S_{\mathrm{s}}.$$

Let $N_{\mathrm{m}} = M_{\mathrm{s}} + M_i$ and $N_{\mathrm{s}} = S_{\mathrm{s}} + S_i$. From system (1), we have

$$\dot{N}_{\mathrm{m}} \le r_{\mathrm{m}} M_s \left(1 - \frac{M_{\mathrm{s}}}{K_{\mathrm{m}}}\right) - d_{\mathrm{m}} N_{\mathrm{m}} - \mu_{\mathrm{m}} M_i \le \frac{1}{4} r_{\mathrm{m}} K_{\mathrm{m}} - d_{\mathrm{m}} N_{\mathrm{m}},$$
$$\dot{N}_{\mathrm{s}} \le r_{\mathrm{s}} S_{\mathrm{s}} \left(1 - \frac{S_{\mathrm{s}}}{K_{\mathrm{s}}}\right) - d_{\mathrm{s}} N_{\mathrm{s}} - \mu_{\mathrm{s}} S_i \le \frac{1}{4} r_{\mathrm{s}} K_{\mathrm{s}} - d_{\mathrm{s}} N_{\mathrm{s}}.$$

Therefore, all the solutions in the nonnegative cone approach, enter, or stay inside the region.

$$\Sigma = \left\{ 0 \le M_{\mathrm{s}} \le U_1, 0 \le S_{\mathrm{s}} \le U_2, 0 \le N_{\mathrm{m}} \le \frac{r_{\mathrm{m}} K_{\mathrm{m}}}{4 d_{\mathrm{m}}}, 0 \le N_{\mathrm{s}} \le \frac{r_{\mathrm{s}} K_{\mathrm{s}}}{4 d_{\mathrm{s}}} \right\},$$

where $U_1 = \max\{0, \frac{K_{\mathrm{m}}(r_{\mathrm{m}} - d_{\mathrm{m}})}{r_{\mathrm{m}}}\}$ and $U_2 = \max\{0, \frac{K_{\mathrm{s}}(r_{\mathrm{s}} - d_{\mathrm{s}})}{r_{\mathrm{s}}}\}$. □

3 Dynamics of the Model

3.1 Existence of Equilibria

System (1) has at most four equilibria on the boundary of the nonnegative cone: $E_0 = (0, 0, 0, 0)$, representing the extinction of both species; $E_{b1} = (\frac{K_m(r_m - d_m)}{r_m}, 0, 0, 0)$, representing the extinction of the snails and existence of the mice; $E_{b2} = (0, 0, \frac{K_s(r_s - d_s)}{r_s}, 0)$, representing the extinction of the mice and existence of the snails; and $E_{DFE} = (\frac{K_m(r_m - d_m)}{r_m}, 0, \frac{K_s(r_s - d_s)}{r_s}, 0)$, representing the coexistence of both species in the absence of disease.

According to the next generation matrix method (van den Driessche and Watmough 2002), we calculate the basic reproduction number

$$\mathscr{R}_0 = \sqrt{\frac{\beta_m K_m (r_m - d_m)}{r_m (d_m + \mu_m)} \frac{\beta_s K_s (r_s - d_s)}{r_s (d_s + \mu_s)}}. \tag{2}$$

$\mathscr{R}_0$ is well defined if $r_m > d_m$ and $r_s > d_s$. If $r_m \le d_m$ or $r_s \le d_s$, then either mice or snails will be extinct, and the disease cannot outbreak. From now on, we study system (1) when $\mathscr{R}_0$ is well defined. One can obtain the following proposition based on the standard stability analysis.

Proposition 3.1 *For system* (1)*,*

Equilibrium	$r_m < d_m, r_s < d_s$	$r_m > d_m, r_s > d_s$		
		$R_0 < 1$	$R_0 = 1$	$R_0 > 1$
E_0	*stablenode*	*saddle*	*saddle*	*saddle*
E_{b1}	*notexist*	*saddle*	*saddle*	*saddle*
E_{b2}	*notexist*	*saddle*	*saddle*	*saddle*
E_{DFE}	*notexist*	*stablenode*	*saddle-node*	*saddle*

For any endemic equilibrium, one can find that its coordinates should satisfy

$$\begin{cases} M_i = g_1(S_i) \triangleq \overbrace{\dfrac{\beta_m}{d_m + \mu_m} \dfrac{K_m}{r_m} \beta_m}^{C} \left(\overbrace{\dfrac{r_m - d_m}{\beta_m}}^{D} - S_i \right) S_i, \\ S_i = g_2(M_i) \triangleq \underbrace{\dfrac{\beta_s}{d_s + \mu_s} \dfrac{K_s}{r_s} \beta_s}_{A} \left(\underbrace{\dfrac{r_s - d_s}{\beta_s}}_{B} - M_i \right) M_i. \end{cases} \tag{3}$$

Eliminating the variable S_i in (3), we can obtain the following cubic equation with respect to M_i:

$$G(M_i) := A^2CM_i^3 - 2A^2BCM_i^2 + (A^2B^2C + ACD)M_i + 1 - \mathscr{R}_0^2 = 0. \quad (4)$$

For the existence of the endemic equilibrium point, we have the following proposition.

Proposition 3.2 *If $\mathscr{R}_0 \leq 1$, there is no endemic equilibrium; If $\mathscr{R}_0 > 1$, then there will be at least one endemic equilibrium and three endemic equilibria at most.*

Proof Two parabolas $M_i = g_1(S_i)$ and $S_i = g_2(M_i)$ have no intersection in the first quadrant of (M_i, S_i) plane if and only if $\frac{\partial g_2(M_i)}{\partial M_i}(0) \leq (\frac{\partial g_1(S_i)}{\partial S_i}(0))^{-1}$, which is equivalent to $\mathscr{R}_0 \leq 1$. Therefore, there is no endemic equilibrium if $\mathscr{R}_0 \leq 1$.

If $\mathscr{R}_0 > 1$, then $G(0) = 1 - \mathscr{R}_0^2 < 0$. By intermediate value theorem, equation (4) has at least one positive root. Equation (4) has at most three positive roots according to the fundamental theorem of algebra, so system (1) has at most three endemic equilibria. □

Proposition 3.3 *If $\mathscr{R}_0 < 1$, then* $\lim_{t\to+\infty} \begin{pmatrix} M_i(t) \\ S_i(t) \end{pmatrix} = 0$ *for* $\forall\ (M_s(0), M_i(0), S_s(0), S_i(0)) \in \overline{R^{4+}}$.

Proof From proposition 2.1, we can restrict our analysis in region Σ.

Let $Q = \begin{pmatrix} -(d_m + \mu_m) & \frac{\beta_m K_m (r_m - d_m)}{r_m} \\ \frac{\beta_s K_s (r_s - d_s)}{r_s} & -(d_s + \mu_s) \end{pmatrix}$. Since $\mathscr{R}_0 < 1$, one can verify that all the eigenvalues of Q have negative real parts. The variation of constant formula yields to

$$\begin{aligned} 0 \leq \begin{pmatrix} M_i(t) \\ S_i(t) \end{pmatrix} &= e^{Qt} \begin{pmatrix} M_i(0) \\ S_i(0) \end{pmatrix} - \int_0^t e^{Q(t-\tau)} \begin{pmatrix} \beta_m S_i \left(\frac{K_m (r_m - d_m)}{r_m} - M_s(\tau) \right) \\ \beta_s M_i \left(\frac{K_s (r_s - d_s)}{r_s} - S_s(\tau) \right) \end{pmatrix} d\tau \\ &\leq e^{Qt} \begin{pmatrix} M_i(0) \\ S_i(0) \end{pmatrix} \longrightarrow 0 \ (t \to +\infty). \end{aligned}$$

Therefore, the disease is eradicated when $\mathscr{R}_0 < 1$. □

Define $\Sigma_1 = \Sigma \cap \{M_i = S_i = 0\}$. From Proposition 3.3, if $\mathscr{R}_0 < 1$, then we only need to analyze system (1) in the region Σ_1 by the limit system theory.

Let $\Sigma_{b1} = \Sigma \cap \{M_i = S_i = S_s = 0\}$ and $\Sigma_{b2} = \Sigma \cap \{M_i = S_i = M_s = 0\}$. In Σ_1, two equilibrium points E_{b1} and E_{b2} are saddles with the stable manifold in Σ_{b1} and Σ_{b2}, respectively, and E_0 is a repelling node. There is no limit cycle in Σ_1, which can be proved by contradiction. Hence, we can obtain the following proposition.

Proposition 3.4 *If $\mathscr{R}_0 < 1$, then E_{DFE} is globally asymptotically stable in $\Sigma_1 \setminus (\Sigma_{b1} \bigcup \Sigma_{b2})$.*

Recall that $K_m = k_m K$ and $K_s = k_s K$, where K is the area of islet, and from (2), we have $\mathscr{R}_0 = K\sqrt{\frac{\beta_m k_m (r_m - d_m)}{r_m (d_m + \mu_m)} \frac{\beta_s k_s (r_s - d_s)}{r_s (d_s + \mu_s)}}$. Hence, given the demographic parameters and contact transmission rates, $\mathscr{R}_0$ is proportional to the size K of the islet.

Let $\mathscr{R}_0 = 1$, we have

$$K_c = \sqrt{\frac{r_m(d_m + \mu_m)}{\beta_m k_m (r_m - d_m)} \frac{r_s(d_s + \mu_s)}{\beta_s k_s (r_s - d_s)}}. \tag{5}$$

It is the threshold size of the islet for the prevalence of the disease. From Proposition 3.2 and Proposition 3.3, if $K < K_c$, then the disease will die out; if $K > K_c$, then the disease will outbreak.

According to the existence of the equilibrium and the stability analysis in Proposition 3.1 and Proposition 3.2, the steady state bifurcations outlined below occur.

Theorem 3.5 *(i) System (1) undergoes a transcritical bifurcation involving E_0 and E_{b1} (or E_{b2}) when $r_m = d_m$ (or $r_s = d_s$), and E_0 changes its stability from an attracting node to a saddle while increasing the parameter r_m (or r_s).*

(ii) System (1) undergoes a transcritical bifurcation involving E_{DFE} and an endemic equilibrium point when $\mathscr{R}_0 = 1$, and E_{DFE} changes its stability from an attracting node to a saddle point while increasing $\mathscr{R}_0$.

3.2 Stability and Bifurcations

In this section, we study the stability of endemic equilibria and possible bifurcations under the condition $\mathscr{R}_0 > 1$. Denote any endemic equilibrium point as $\bar{E} = (\bar{M}_s, \bar{M}_i, \bar{S}_s, \bar{S}_i)$. The Jacobian at $\bar{E}$ is given by

$$T = \begin{pmatrix} -\frac{r_m}{K_m}\bar{M}_s & 0 & 0 & -\beta_m \bar{M}_s \\ \beta_m \bar{S}_i & -(d_m + \mu_m) & 0 & \beta_m \bar{M}_s \\ 0 & -\beta_s \bar{S}_s & -\frac{r_s}{K_s}\bar{S}_s & 0 \\ 0 & \beta_s \bar{S}_s & \beta_s \bar{M}_i & -(d_s + \mu_s) \end{pmatrix},$$

so the eigenvalues of T are the roots of

$$\lambda^4 + p_3\lambda^3 + p_2\lambda^2 + p_1\lambda + p_0 = 0, \tag{6}$$

where

$$p_0 = (d_m + \mu_m)(d_s + \mu_s)\left(\frac{r_m \beta_s}{K_m}\bar{M}_s\bar{M}_i + \frac{r_s \beta_m}{K_s}\bar{S}_s\bar{S}_i - \beta_m\beta_s\bar{M}_i\bar{S}_i\right),$$

$$p_1 = \frac{r_m}{K_m}\frac{r_s}{K_s}\bar{M}_s\bar{S}_s(d_m + \mu_m + d_s + \mu_s) + (\beta_m\bar{S}_i + \beta_s\bar{M}_i)(d_m + \mu_m)(d_s + \mu_s) > 0,$$

$$p_2 = \frac{r_m}{K_m}\bar{M}_s\frac{r_s}{K_s}\bar{S}_s + \left(\frac{r_m}{K_m}\bar{M}_s + \frac{r_s}{K_s}\bar{S}_s\right)(d_m + \mu_m + d_s + \mu_s) > 0,$$

$$p_3 = \frac{r_m}{K_m}\bar{M}_s + \frac{r_s}{K_s}\bar{S}_s + d_m + \mu_m + d_s + \mu_s > 0.$$

Since $p_1 > 0$, the characteristic equation (6) cannot have double-zero eigenvalues; then, the Bogdanov-Takens bifurcation and $1 : q$ ($q \in N$) resonance bifurcation cannot occur. System (1) cannot present the Hopf-Hopf bifurcation, because the characteristic equation (6) does not have two pairs of pure imaginary roots due to $p_3 > 0$. The Lemma 3.6 in section 3.2.1 asserts that the cusp bifurcation and the Hopf bifurcation cannot happen simultaneously. Therefore, as the breakthrough point, we study the cusp bifurcation which is related to the bifurcation of the equilibria, and then study the Hopf bifurcation which can change the stability of the equilibria and induce oscillations.

3.2.1 Cusp Bifurcation of Codimension 2

It is impossible to solve (4) to get the equilibrium or study its stability from (6). Alternatively, from the viewpoint of bifurcation, we first study the singularity with multiplicity 3, and then obtain the existence and stability of all the possible equilibria from the bifurcation analysis.

A dynamical system restricted on the center manifold is generally of lower dimension than the original system, and the center manifold theorem (Carr 1981) shows that qualitative behaviors in a neighborhood of a non-hyperbolic critical point are determined by its behaviors on the center manifold. There are no theoretical difficulties in the center manifold calculation, but calculations are very complicated in higher or infinite dimensional systems, and that is the reason why the bifurcation analyses of high codimension are directly carried out for the planar system in most papers. The high dimension of model (1) brings more difficulties that we cannot easily transform the linear part of the system into a canonical form.

The projection technique, derived from the adjoint operator and spectral decomposition theory, avoiding changing the linear part into a canonical form, was originally developed to study bifurcations in partial differential equations using the Lyapunov–Schmidt reduction. With this technique, Hassard et al. studied the center manifold and normal form of Hopf bifurcation in finite and infinite dimensional systems Hassard et al. (1981). Here, we apply this technique to the center manifold computation, because we have no idea about the other three eigenvalues except the sign of their real parts as shown in Lemma 3.6.

The endemic equilibrium of multiplicity 3 implies that

$$g(M_i) = g'(M_i) = g''(M_i) = 0. \tag{7}$$

From the above equations, we obtain this critical equilibrium point.

$$E^* = (M_{\mathrm{s}}^*, M_i^*, S_{\mathrm{s}}^*, S_i^*) = \left(\frac{d_{\mathrm{m}} + \mu_{\mathrm{m}}}{\beta_{\mathrm{m}}} \frac{3}{AB}, \frac{2B}{3}, \frac{d_{\mathrm{s}} + \mu_{\mathrm{s}}}{\beta_{\mathrm{s}}} \frac{AB}{3}, \frac{2AB^2}{9} \right).$$

It follows from (4) and (7) that the parameters of model (1) in this case should satisfy

$$AB^2 - 3D = 0, \quad A^2B^3C - 27 = 0, \tag{8}$$

and we have the following lemma.

Lemma 3.6 *For the endemic equilibrium E^*, $\lambda = 0$ is a simple eigenvalue, and all other eigenvalues have negative real parts.*

Proof Let $g(\lambda) = \lambda^4 + p_3\lambda^3 + p_2\lambda^2 + p_1\lambda + p_0$. For the endemic equilibrium E^*, we have $g(0) = p_0 = 0$, and $g'(0) = p_1 > 0$, so $\lambda = 0$ is a simple root of $g(\lambda) = 0$. Furthermore, $p_3 > 0$ and $p_2p_3 - p_1 > 0$. By Routh-Hurwitz criteria, we prove the lemma. □

From conditions (8), by means of Implicit Function Theorem, there exist two smooth functions $K^* = K^*(r_\mathrm{m}, r_\mathrm{s}, \beta_\mathrm{m}, \beta_\mathrm{s}, \mu_\mathrm{m}, \mu_\mathrm{s}, k_\mathrm{m}, k_\mathrm{s}, d_\mathrm{s})$ and $d_\mathrm{m}^* = d_\mathrm{m}^*(r_\mathrm{m}, r_s, \beta_\mathrm{m}, \beta_\mathrm{s}, \mu_\mathrm{m}, \mu_\mathrm{s}, k_\mathrm{m}, k_\mathrm{s}, d_\mathrm{s})$. When $K = K^*$ and $d_\mathrm{m} = d_\mathrm{m}^*$, three endemic equilibria coalesce at E^*. In the following, we prove that E^* is a cusp bifurcation point of codimension 2, and use a series of transformations to reduce system (1) to the normal form, by which the bifurcation and dynamics of system (1) will be presented. First, we need the following preliminaries.

Lemma 3.7 *Let*

$$\phi = \left(-\frac{\beta_\mathrm{m}K_\mathrm{m}}{r_\mathrm{m}}, -\frac{\beta_\mathrm{m}K_\mathrm{m}(r_\mathrm{m} - d_\mathrm{m})}{r_\mathrm{m}(d_\mathrm{m} + \mu_\mathrm{m})}, \frac{3(d_\mathrm{s} + \mu_\mathrm{s})}{r_\mathrm{s} - d_\mathrm{s}}, 1\right)',$$
$$\Psi = \left(-\frac{2\beta_\mathrm{s}K_\mathrm{s}(r_\mathrm{s} - d_\mathrm{s})}{3r_\mathrm{s}(d_\mathrm{m} + \mu_\mathrm{m})}, -\frac{\beta_\mathrm{s}K_\mathrm{s}(r_\mathrm{s} - d_\mathrm{s})}{3r_\mathrm{s}(d_\mathrm{m} + \mu_\mathrm{m})}, 2, 1\right)',$$

$\alpha = \langle\Psi, \phi\rangle^{-1}$, and $\Phi = \alpha\phi$; then Φ and Ψ are the eigenvectors corresponding to $\lambda = 0$ of T and T^* which satisfy $\langle\Psi, \Phi\rangle = 1$. Here, $\langle\cdot, \cdot\rangle$ is the inner product in R^4 and T^* is the adjoint operator of T.

Define the space $T^{\mathrm{su}} = \{Y \in R^4 | \langle\Psi, Y\rangle = 0\}$, and then we have the following theorem.

Theorem 3.8 *For system (1),*

(i) The endemic equilibrium E^* is a cusp bifurcation point of codimension 2.
(ii) The endemic equilibrium E^* is a stable equilibrium.

Proof *(i)* It has been shown in Chow et al. (1994), Kuznetsov (1998) that any system which has a cusp bifurcation point of codimension 2 is C^∞ equivalent to

$$\dot{u} = -u^3 + o(u^3). \tag{9}$$

Thus, it is sufficient to show that there exist smooth coordinate changes which transform system (1) into (9) on the center manifold with conditions (8). The translation

$$x_1 = M_\mathrm{s} - M_\mathrm{s}^*, x_2 = M_i - M_i^*, x_3 = S_\mathrm{s} - S_\mathrm{s}^*, x_4 = S_i - S_i^*, \tag{10}$$

brings E^* to the origin, and we obtain $\dot{X} = TX + f(X)$, where $X = (x_1, x_2, x_3, x_4)'$ and

$$f(X) = \left(-\frac{r_{\mathrm{m}}}{K_{\mathrm{m}}} x_1^2 - \beta_{\mathrm{m}} x_1 x_4, \beta_{\mathrm{m}} x_1 x_4, -\frac{r_{\mathrm{s}}}{K_{\mathrm{s}}} x_3^2 - \beta_s x_2 x_3, \beta_s x_2 x_3 \right)'.$$

Using the Fredholm Alternative Theorem, we can decompose any vector $X \in R^4$ as $X = u\Phi + Y$ with

$$\begin{cases} u = \langle \Psi, X \rangle, \\ Y = X - \langle \Psi, X \rangle \Phi. \end{cases}$$

The scalar u and vector $Y \in T^{\mathrm{su}}$ can be considered as new coordinates, and system (1) can be written as

$$\begin{cases} \dot{u} = \langle \Psi, f(u\Phi + Y) \rangle, \\ \dot{Y} = TY + f(u\Phi + Y) - \langle \Psi, f(u\Phi + Y) \rangle \Phi. \end{cases} \tag{11}$$

From Lemma 3.6 and the center manifold theorem, there exists a one-dimensional center manifold of system (11) which can be represented as follows:

$$W^c(0) = \{(u, Y) \in (R, T^{su}) | Y = h(u), |u| < \delta, h(0) = 0, Dh(0) = 0\}$$

for δ sufficiently small. Hence, $h(u) = au^2 + O(u^3)$, which satisfies

$$Dh(u)(\langle \Psi, f(u\Phi + Y) \rangle) = TY + f(u\Phi + h(u)) - \langle \Psi, f(u\Phi + h(u)) \rangle \Phi, \tag{12}$$

where $a = (a_1, a_2, a_3, a_4)' \in T^{su} \subset R^4$, which will be determined later. Therefore, system (1) restricted on the center manifold is given by

$$\begin{aligned} \dot{u} = & -\left(\frac{r_{\mathrm{m}}}{K_{\mathrm{m}}} \psi_1 \phi_1^2 + \beta_m \psi_2 \phi_1 \phi_4 + \frac{r_{\mathrm{s}}}{K_{\mathrm{s}}} \psi_3 \phi_3^2 + \beta_{\mathrm{s}} \psi_4 \phi_2 \phi_3 \right) u^2 \\ & - \left[2 \left(\frac{r_{\mathrm{m}}}{K_{\mathrm{m}}} \psi_1 \phi_1 a_1 + \frac{r_{\mathrm{s}}}{K_{\mathrm{s}}} \psi_3 \phi_3 a_3 \right) + \beta_{\mathrm{m}} \psi_2 (\phi_1 a_4 + \phi_4 a_1) \right. \\ & \left. + \beta_{\mathrm{s}} \psi_4 (\phi_2 a_4 + \phi_3 a_2) \right] u^3 + o(u^3). \end{aligned} \tag{13}$$

Here, ψ_i and ϕ_i $(i = 1, 2, 3, 4)$ are the ith components of the vectors Ψ and Φ, respectively. Comparing the coefficients of each power of u from both sides of equation (12), we obtain

$$Ta = \begin{pmatrix} 0 \\ -\beta_{\mathrm{m}} \phi_1 \phi_4 \\ 0 \\ -\beta_{\mathrm{s}} \phi_2 \phi_3 \end{pmatrix} \Rightarrow a = (I - \Phi \Psi') \begin{pmatrix} 0 \\ -\alpha^2 C \\ 27\alpha^2 \frac{d_{\mathrm{s}} + \mu_{\mathrm{s}}}{\beta_{\mathrm{s}} A B^3} \\ 0 \end{pmatrix},$$

where $I \in R^{4\times 4}$ is a unit matrix. Substituting a into (13), we obtain the reduced system on the center manifold

$$\dot{u} = -\frac{6\alpha^3(d_s + \mu_s)C}{B}u^3 + o(u^3). \tag{14}$$

The coefficient of u^3 is negative since $\alpha = \langle \Psi, \phi \rangle^{-1} > 0$. Hence, E^* is a cusp bifurcation point of codimension 2.

(ii) From (14), one can see that E^* is stable on the center manifold, and according to Lemma 3.6, E^* is a stable equilibrium. □

By Theorem 3.8, if $K = K^*$ and $d_m = d_m^*$, then the endemic equilibrium E^* is a cusp bifurcation point of codimension 2. In order to investigate the impact of the expansion of the islet and design control strategies on schistosomiasis transmission, we take (K, d_m) as bifurcation parameters and develop a generic unfolding of the cusp bifurcation for system (1), when (K, d_m) is perturbed near the point (K^*, d_m^*). Substituting

$$\begin{cases} K = K^* + \epsilon_1, \\ d_m = d_m^* + \epsilon_2, \end{cases} \tag{15}$$

into system (1), we obtain the perturbed system

$$\begin{cases} \dot{M}_s = r_m M_s \left(1 - \frac{M_s}{k_m(K^*+\epsilon_1)}\right) - (d_m^* + \epsilon_2)M_s - \beta_m M_s S_i, \\ \dot{M}_i = \beta_m M_s S_i - (d_m + \mu_m)M_i, \\ \dot{S}_s = r_s S_s \left(1 - \frac{S_s}{k_s(K^*+\epsilon_1)}\right) - d_s S_s - \beta_s M_i S_s, \\ \dot{S}_i = \beta_s M_i S_s - (d_s + \mu_s)S_i, \end{cases} \tag{16}$$

where $\epsilon = (\epsilon_1, \epsilon_2)$ is sufficiently small.

Theorem 3.9 *For the parameter $\epsilon = (\epsilon_1, \epsilon_2)$ sufficiently small, system (16) is a generic unfolding of the cusp bifurcation of codimension 2.*

The unfolding of codimension 2 cusp bifurcation is given in the bifurcation diagram of Fig. 2 with parameters K and d_m.

Proof It has been shown in Chow et al. (1994), Kuznetsov (1998) that a generic unfolding with parameters (ν_0, ν_1) of codimension 2 cusp bifurcation is C^∞ equivalent to

$$\dot{v} = \nu_0 + \nu_1 v - v^3, \tag{17}$$

so we will prove that system (16) with the parameter (ϵ_1, ϵ_2) is also a generic unfolding of codimension 2 cusp bifurcation by showing that there exist smooth coordinate changes which take system (16) into (17) on the center manifold. Applying the translation (10) and expanding system (16) in the power series at origin, we have

$$\begin{cases} \dot{X} = TX + F(X, \epsilon), \\ \dot{\epsilon} = 0, \end{cases} \tag{18}$$

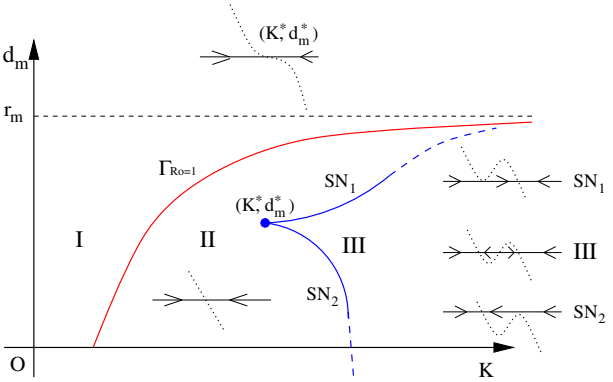

Fig. 2 Bifurcation diagram in the (K, d_{m}) plane and the phase portrait on the one-dimensional center manifold in a small neighborhood of (K^*, d_{m}^*) (Color figure online)

$$\text{and} \quad F(X,\epsilon) = \begin{pmatrix} -M_{\mathrm{s}}^*\epsilon_2 - \frac{r_{\mathrm{m}}x_1^2}{K_{\mathrm{m}}^*} - \beta_{\mathrm{m}}x_1x_4 - \epsilon_2x_1 + \frac{r_{\mathrm{m}}\epsilon_1(M_{\mathrm{s}}^{*2}+2M_{\mathrm{s}}^*x_1+x_1^2)}{K_{\mathrm{m}}^*K^*} \\ -M_i^*\epsilon_2 + \beta_{\mathrm{m}}x_1x_4 - \epsilon_2x_2 \\ -\frac{r_{\mathrm{s}}x_3^2}{K_{\mathrm{s}}^*} - \beta_s x_2x_3 + \frac{r_{\mathrm{s}}\epsilon_1(S_{\mathrm{s}}^{*2}+2S_{\mathrm{s}}^*x_3+x_3^2)}{K_{\mathrm{s}}^*K^*} \\ \beta_{\mathrm{s}}x_2x_3 \end{pmatrix} + O(|\epsilon|^2, |\epsilon|^2X, |\epsilon|^2X^2),$$

where $K_{\mathrm{m}}^* = k_{\mathrm{m}}K^*$ and $K_{\mathrm{s}}^* = k_{\mathrm{s}}K^*$. Following the same procedure in Theorem 3.8, system (18) can be written as

$$\begin{cases} \dot{u} = \langle \Psi, F(u\Phi + Y)\rangle, \\ \dot{Y} = TY + F(u\Phi + Y) - \langle \Psi, F(u\Phi + Y)\rangle\Phi, \\ \dot{\epsilon} = 0, \end{cases} \tag{19}$$

and the center manifold has the representation

$$Y = h(u,\epsilon_1,\epsilon_2) = c_1\epsilon_1 + c_2\epsilon_2 + au^2 + b_1u\epsilon_1 + b_2u\epsilon_2 + O(|\epsilon_1,\epsilon_2|^2) + O(|u,\epsilon_1,\epsilon_2|^3).$$

Since

$$D_uh(u,\epsilon_1,\epsilon_2)\dot{u} + D_{\epsilon_1}h(u,\epsilon_1,\epsilon_2)\dot{\epsilon_1} + D_{\epsilon_2}h(u,\epsilon_1,\epsilon_2)\dot{\epsilon_2} = Dh(u)(\langle \Psi, F(u\Phi + h(u,\epsilon_1,\epsilon_2))\rangle),$$

$h(u,\epsilon_1,\epsilon_2)$ should satisfy

$$Dh(u)(\langle\Psi, F(u\Phi + h(u,\epsilon_1,\epsilon_2))\rangle) = Th(u,\epsilon_1,\epsilon_2) + F(u\Phi + h(u,\epsilon_1,\epsilon_2)) - \langle\Psi, F(u\Phi + h(u,\epsilon_1,\epsilon_2))\rangle\Phi, \tag{20}$$

where $a, b_1, b_2, c_1, c_2 \in T^{\mathrm{su}} \subset R^4$, and $\cdot = \mathrm{d}/\mathrm{d}t$.

According to the equation (20), we have

$$Ta = \zeta_0,\ Tc_1 = \zeta_1,\ \text{ and }\ Tc_2 = \zeta_2, \tag{21}$$

where

$$\zeta_0 = \begin{pmatrix} 0 \\ -\beta_{\mathrm{m}}\phi_1\phi_4 \\ 0 \\ -\beta_{\mathrm{s}}\phi_2\phi_3 \end{pmatrix}, \quad \zeta_1 = \begin{pmatrix} -\frac{(d_{\mathrm{s}}+\mu_{\mathrm{s}})AB^2}{9K^*} \\ 0 \\ -\frac{(d_{\mathrm{m}}+\mu_{\mathrm{m}})B}{3K^*} \\ 0 \end{pmatrix},$$

$$\zeta_2 = \begin{pmatrix} -\phi_1(\psi_1 M_{\mathrm{s}}^* + \psi_2 M_i^*) + M_{\mathrm{s}}^* \\ -\phi_2(\psi_1 M_{\mathrm{s}}^* + \psi_2 M_i^*) + M_i^* \\ -\phi_3(\psi_1 M_{\mathrm{s}}^* + \psi_2 M_i^*) \\ -\phi_4(\psi_1 M_{\mathrm{s}}^* + \psi_2 M_i^*) \end{pmatrix}.$$

By solving linear systems (21), we obtain that

$$a = (I - \Phi\Psi')\begin{pmatrix} 0 \\ -\alpha^2 C \\ \frac{27\alpha^2(d_{\mathrm{s}}+\mu_{\mathrm{s}})}{\beta_{\mathrm{s}}AB^3} \\ 0 \end{pmatrix}, \qquad c_1 = (I - \Phi\Psi')\frac{1}{K^*}\begin{pmatrix} M_s^* \\ M_i^* \\ -S_s^* \\ 0 \end{pmatrix},$$

$$c_2 = (I - \Phi\Psi') \times \begin{pmatrix} \frac{K_{\mathrm{m}}^*}{r_{\mathrm{m}}}\left(\psi_1\phi_1 - 1 + \psi_2\phi_1\frac{M_i^*}{M_{\mathrm{s}}^*}\right) \\ \frac{1}{d_{\mathrm{m}}+\mu_{\mathrm{m}}}\left[\frac{K_{\mathrm{m}}^*\beta_{\mathrm{m}}S_i^*}{r_{\mathrm{m}}}\left(\psi_1\phi_1 - 1 + \psi_2\phi_1\frac{M_i^*}{M_{\mathrm{s}}^*}\right) + \phi_2(\psi_1 M_{\mathrm{s}}^* + \psi_2 M_i^*) - M_i^*\right] \\ -\frac{3((\psi_1\phi_3+\psi_1\phi_4)M_{\mathrm{s}}^* + (\psi_2\phi_3+\psi_2\phi_4)M_i^*)}{\beta_{\mathrm{s}}B} \\ 0 \end{pmatrix}.$$

Substituting a, c_1, and c_2 into the first equation of (19), we obtain

$$\dot{u} = \mu_0(\epsilon_1,\epsilon_2) + \mu_1(\epsilon_1,\epsilon_2)u + \mu_2(\epsilon_1,\epsilon_2)u^2 + \mu_3(\epsilon_1,\epsilon_2)u^3 + O(u^4), \tag{22}$$

where

$$\mu_0(\epsilon_1,\epsilon_2) = \left(\frac{2(d_{\mathrm{s}}+\mu_{\mathrm{s}})}{\beta_{\mathrm{m}}} + \frac{2K_{\mathrm{s}}^*(r_{\mathrm{s}}-d_{\mathrm{s}})^2}{(d_{\mathrm{m}}^*+\mu_{\mathrm{m}})r_{\mathrm{s}}}\right)\epsilon_2 + O(|\epsilon_1,\epsilon_2|^2),$$

$$\mu_1(\epsilon_1,\epsilon_2) = 6\alpha\frac{d_{\mathrm{s}}+\mu_{\mathrm{s}}}{K^*}\epsilon_1 + \tilde{C}_0\epsilon_2 + O(|\epsilon_1,\epsilon_2|^2),$$

$$\mu_2(\epsilon_1,\epsilon_2) = O(|\epsilon_1,\epsilon_2|),$$
$$\mu_3(\epsilon_1,\epsilon_2) = -6\alpha^3(d_s+\mu_s)\frac{C}{B} + O(|\epsilon_1,\epsilon_2|),$$

and

$$\tilde{C}_0 = -\alpha^2(d_s+\mu_s)\left[\frac{63(d_s+\mu_s)}{AB^2(d_m^*+\mu_m)\beta_m} + \frac{12(d_s+\mu_s)}{d_m^*+\mu_m\beta_s B} + \frac{324(d_s+\mu_s)}{\beta_m^2 A^2 B^4} + \frac{d_s+\mu_s}{(d_m^*+\mu_m)^2} + \frac{5}{d_m^*+\mu_m} + \frac{27}{\beta_m AB^2}\right] < 0.$$

Let $v = -\mu_3^{\frac{1}{3}}u - \frac{1}{3}\mu_2\mu_3^{-\frac{2}{3}}$. This translation brings system (22) to

$$\dot{v} = \nu_0(\epsilon_1,\epsilon_2) + \nu_1(\epsilon_1,\epsilon_2)v - v^3 + O(v^4), \tag{23}$$

where

$$\nu_0(\epsilon_1,\epsilon_2) = \mu_0 + \frac{2\mu_2^3}{27\mu_3^2} - \frac{\mu_1\mu_2}{3\mu_3} = \xi_0\epsilon_2 + O(|\epsilon_1,\epsilon_2|^2),$$
$$\nu_1(\epsilon_1,\epsilon_2) = -\frac{\mu_1}{\mu_3^{1/3}} + \frac{\mu_2^2}{3\mu_3^{4/3}} = \xi_1\epsilon_1 + \xi_2\epsilon_2 + O(|\epsilon_1,\epsilon_2|^2),$$

and

$$\xi_0 = \frac{2(d_s+\mu_s)}{\beta_m} + \frac{2K_s^*(r_s-d_s)^2}{(d_m^*+\mu_m)r_s} > 0,$$
$$\xi_1 = \frac{(6(d_s+\mu_s))^{\frac{2}{3}}}{K^*\left(\frac{C}{B}\right)^{\frac{1}{3}}} > 0, \quad \xi_2 = \frac{\tilde{C}_0}{\alpha\left(6(d_s+\mu_s)\frac{C}{B}\right)^{\frac{1}{3}}} < 0.$$

Therefore,

$$\frac{\partial(\nu_0,\nu_1)}{\partial(\epsilon_1,\epsilon_2)}_{|\epsilon=(0,0)} = -\xi_0\xi_1 \neq 0.$$

Using the Malgrange Preparation Theorem, system (23) is topologically equivalent to

$$\dot{v} = \nu_0(\epsilon_1,\epsilon_2) + \nu_1(\epsilon_1,\epsilon_2)v - v^3.$$

Hence, system (16) with parameter $\epsilon = (\epsilon_1,\epsilon_2)$ is a generic unfolding of codimension 2 cusp bifurcation. □

From Theorem 3.9, one can immediately obtain the following corollary.

Corollary 3.10 *For system (1), the saddle-node bifurcation and pitchfork bifurcation can occur. Furthermore, two branches of saddle-node bifurcation curves intersecting at (K^*, d_{m}^*) can be represented in terms of K and d_m as follows:*

$$SN_{1,2} = \left\{ (K, d_{\mathrm{m}}) | \xi_0 (d_{\mathrm{m}} - d_{\mathrm{m}}^*) = \pm \sqrt{\frac{4}{27} (\xi_1 (K_{\mathrm{m}} - K_{\mathrm{m}}^*) + \xi_2 (d_{\mathrm{m}} - d_{\mathrm{m}}^*))^3} + O(|\epsilon_1, \epsilon_2|^2) \right\}.$$

3.2.2 Hopf Bifurcation

In this section, we study the Hopf bifurcation. Since $p_3 > 0$, the characteristic equation (6) cannot have two pairs of pure imaginary roots simultaneously, so the Hopf-Hopf bifurcation cannot occur. We choose K as the bifurcation parameter, then coefficients p_1, p_2, p_3, and p_4 are functions of K. Let

$$\varphi(K) = (p_2(K) p_3(K) - p_1(K)) p_1(K) - p_3^2(K) p_0(K).$$

Theorem 3.11 *Suppose there exists a $\widetilde{K} > 0$ such that $p_0(\widetilde{K}) > 0$, $\varphi(\widetilde{K}) = 0$ and $\frac{\mathrm{d}\varphi(K)}{\mathrm{d}K}\big|_{K=\widetilde{K}} \neq 0$, then the Hopf bifurcation occurs and a family of periodic solutions appear from the endemic equilibrium point $\bar{E}$ when K passes through $\widetilde{K}$.*

Proof If there exists a $\widetilde{K} > 0$ such that $p_0(\widetilde{K}) > 0$ and $\varphi(\widetilde{K}) = 0$, then

$$p_2(\widetilde{K}) p_3(\widetilde{K}) - p_1(\widetilde{K}) = p_3^2(K) p_0(K) / p_1(K) > 0.$$

Hence, equation (6) has four roots, $\pm i\omega_0$, λ_1, and λ_2, where $\omega_0 = \sqrt{p_1(\widetilde{K}) / p_3(\widetilde{K})}$, $Re(\lambda_1) < 0$, and $Re(\lambda_2) < 0$. To prove the occurrence of Hopf bifurcation at the endemic equilibrium $\bar{E}$, we need to verify the transversality condition.

Consider the roots of (6) as a function of K. When $0 < |K - \widetilde{K}| \ll 1$, equation (6) has four roots, $\alpha(K) \pm i\omega(K)$, $\lambda_1(K)$, and $\lambda_2(K)$, which satisfy $\alpha(\widetilde{K}) = 0$, $\omega(\widetilde{K}) = \omega_0$, $\lambda_1(\widetilde{K}) = \lambda_1$, and $\lambda_2(\widetilde{K}) = \lambda_2$. Substitute $\lambda = \alpha(K) + i\omega(K)$ into equation (6) and differentiate equation (6) with respect to K. Straightforward calculation leads to

$$\frac{\mathrm{d}\alpha(K)}{\mathrm{d}K}\Big|_{K=\widetilde{K}} = -\frac{p_3}{2[(p_2 p_3 - 2p_1)^2 + p_0 p_3^2]} \frac{\mathrm{d}\varphi(K)}{\mathrm{d}K}\Big|_{K=\widetilde{K}}.$$

Therefore,

$$Sign\left\{ \frac{\mathrm{d}\alpha(K)}{\mathrm{d}K}\Big|_{K=\widetilde{K}} \right\} = -Sign\left\{ \frac{\mathrm{d}\varphi(K)}{\mathrm{d}K}\Big|_{K=\widetilde{K}} \right\} \neq 0.$$

Thus, a pair of complex eigenvalues cross the imaginary axis transversally when $K = \widetilde{K}$, and Hopf bifurcation occurs. □

If d_{m} is chosen as the bifurcation parameter, then we will have the similar result as Theorem 3.11. Figure 3a, b in Sect. 4 show that the Hopf bifurcation occurs when considering K and d_{m} as bifurcation parameters, respectively.

3.3 Bifurcation Diagram

In this section, we present the bifurcation diagram in the region $\{(K, d_m)|K > 0, d_{\mathrm{m}} > 0\}$.

First, $d_{\mathrm{m}} = r_{\mathrm{m}}$ defines a dash curve as shown in Fig. 2 across which the transcritical bifurcation occurs according to Theorem 3.5 (i).

Denote $\gamma = \frac{\beta_{\mathrm{m}} k_m \beta_{\mathrm{s}} k_{\mathrm{s}} (r_{\mathrm{s}} - d_{\mathrm{s}})}{r_{\mathrm{m}} r_{\mathrm{s}} (d_{\mathrm{s}} + \mu_{\mathrm{s}})}$. Solve d_{m} in terms of K from the equation $\mathscr{R}_0 = 1$, and we get

$$\Gamma_{\mathscr{R}_0=1} = \left\{ (K, d_{\mathrm{m}}) | d_{\mathrm{m}} = r_{\mathrm{m}} - \frac{r_{\mathrm{m}} + \mu_{\mathrm{m}}}{\gamma K^2 + 1} \right\}.$$

It is a strictly increasing curve of K with a unique inflection $(\frac{1}{\sqrt{3\gamma}}, \frac{1}{4} r_{\mathrm{m}} - \frac{3}{4} \mu_{\mathrm{m}})$ and a horizontal asymptote $d_{\mathrm{m}} = r_{\mathrm{m}}$ as $K \to +\infty$. The transcritical bifurcation occurs when crossing the curve $\Gamma_{\mathscr{R}_0=1}$.

In the following, we determine the position of (K^*, d_{m}^*). Conditions (8) define the following two curves:

$$\Gamma_{\mathscr{R}_0=3} = \left\{ (K, d_{\mathrm{m}}) | d_{\mathrm{m}} = r_{\mathrm{m}} - \frac{9(r_{\mathrm{m}} + \mu_{\mathrm{m}})}{\gamma K^2 + 9} \right\},$$

$$L = \left\{ (K, d_{\mathrm{m}}) | d_{\mathrm{m}} = r_{\mathrm{m}} - \frac{\beta_{\mathrm{m}} k_{\mathrm{s}} (r_{\mathrm{s}} - d_{\mathrm{s}})^2}{(d_{\mathrm{s}} + \mu_{\mathrm{s}}) r_{\mathrm{s}}} K \right\}.$$

$\Gamma_{\mathscr{R}_0=3}$ is a strictly increasing curve of K passing $(0, -\mu_{\mathrm{m}})$ with a horizontal asymptote $d_{\mathrm{m}} = r_{\mathrm{m}}$ as $K \to +\infty$. L is a strictly decreasing straight line passing $(0, r_m)$. Therefore, they intersect at the half parameter plane $K > 0$, and (K^*, d_{m}^*) is the unique intersection point.

$\Gamma_{\mathscr{R}_0=3}$ and L intersect the K-axis at $(K_1, 0)$ and $(K_2, 0)$ with $K_1 = \sqrt{\frac{9\mu_{\mathrm{m}}}{\gamma r_m}}$ and $K_2 = \frac{r_{\mathrm{m}} r_{\mathrm{s}} (d_{\mathrm{s}} + \mu_{\mathrm{s}})}{k_{\mathrm{s}} \beta_{\mathrm{m}} (r_{\mathrm{s}} - d_{\mathrm{s}})^2}$, respectively. If $K_1 < K_2$, then $d_{\mathrm{m}}^* > 0$. If $K_1 \geq K_2$, then $d_{\mathrm{m}}^* \leq 0$, which means that three endemic equilibria cannot coalesce at E^* in reality. Hence, we only consider the case $K_1 < K_2$. Therefore, the location of (K^*, d_{m}^*) is determined, and one can verify that it is under the curve $\Gamma_{\mathscr{R}_0=1}$.

From the Corollary 3.10, we can plot two branches of saddle-node bifurcation curves, and they intersect at (K^*, d_{m}^*). According the above analysis, we obtain the bifurcation diagram in the (K, d_{m}) plane and have the following theorem.

Theorem 3.12 *For system* (1)*, using* (K, d_{m}) *as parameters, the bifurcation diagram is given in Fig. 2.*

(i) $\Gamma_{\mathscr{R}_0=1}$ *and* $\{(K, d_{\mathrm{m}})|d_{\mathrm{m}} = r_{\mathrm{m}}, K > 0\}$ *are transcritical bifurcation curves.*

(ii) *SN_1 and SN_2 are saddle-node bifurcation curves intersecting at the cusp point (K^*, d_m^*). On $SN_{1,2}$, there are two endemic equilibria, one is stable and the other is a saddle-node.*

(iii) *In region* **I**, *there is no endemic equilibrium, and the disease free equilibrium is stable. In region* **II**, *there is only one stable endemic equilibrium. In region* **III**, *there are three endemic equilibria, two of them are stable and the third one is unstable.*

Remark 3.13 If $K_1 > K_2$, (K^*, d_m^*) is located in the fourth quadrant of the parameter space, yet we can still plot the bifurcation diagram as Fig. 2, and the only difference is that the curve SN_1 distinguishes the region **II** and **III**.

Remark 3.14 The bifurcation analysis is local, so the stability of the endemic equilibrium is valid in a neighborhood of (K^*, d_m^*) in Theorem 3.12. The stability of equilibrium changes with the occurrence of other bifurcations, for example the Hopf bifurcation.

From the characteristic equation (6), for the bifurcation of codimension 2 or even higher codimension bifurcation, the possibility of Bogdanov–Takens bifurcation and Hopf–Hopf bifurcation is excluded. However, the degenerate Hopf bifurcation and Zero-Hopf bifurcation could occur when (K, d_m) is far from (K^*, d_m^*). Nevertheless, it is still difficult to prove that theoretically, since it is hard to get the coordinates of the equilibrium and determine the eigenvalues from the cubic equation (4) and quartic equation (6). In Sect. 4, we will take advantage of numerical simulations to get more insights of system (1), and we do see that these types of bifurcations occur.

4 Simulations

In order to investigate the impact of growing islets and design control strategies on schistosomiasis transmission, we regard the physical size of islet K and the natural death rate of mice d_m as parameters. The range of other parameters are listed in Table 1.

We choose parameter values as follows: $k_m = 9$, $k_s = 80$, $r_m = 0.02$, $r_s = 0.03$, $\beta_m = 8.00 \times 10^{-6}$, $\beta_s = 2.25 \times 10^{-5}$, $d_s = 0.0075$, $\mu_m = 0.000608$, and $\mu_s = 0.0195$.

The disease will die out when $d_m \geq 0.02$, so we consider $d_m \in (0, 0.02)$. Using the parameter values listed above, we can easily find the cusp point $(K^*, d_m^*) = (120, 4 \times 10^{-3})$.

(i) Pitchfork bifurcation. We fix $d_m = 4 \times 10^{-3}$ and consider K as a parameter. When $0 < K < 40$, there is no endemic equilibrium. System (1) undergoes transcritical bifurcation when $K = 40$. When $40 < K < 120$, there is only one stable endemic equilibrium denoted as E. The pitchfork bifurcation occurs as K passing through the bifurcation value $K = 120$ with another two stable endemic equilibria bifurcating from E, and the equilibrium E loses its stability and becomes a saddle. As K increases, two stable endemic equilibria will lose their stability and supercritical Hopf bifurcations occur when $K = 257.49$ and $K = 278.94$, respectively. See Fig. 3a.

Table 1 Parameters, interpretations and values of model (1)

Parameter	Description	Range	Reference
K	Area of islet (m^2)	Parameter	
k_m	Maximum mice population (per m^2)	5–15	Xu et al. (1999)
k_s	Maximum snails population (per m^2)	50–100	Xu et al. (1999)
r_m	Intrinsic growth rate of mice (per day)	0.019–0.2	Estimated
r_s	Intrinsic growth rate of snails (per day)	0.01–0.55	Guo (1991), Liang et al. (2002)
β_m	Contact transmission rate from snails to mice	0.0000005–0.001	Estimated
β_s	Contact transmission rate from mice to snails	0.000001–0.0005	Spear et al. (2002)
d_m	Nature death rate of mice (per day)	Parameter	
d_s	Nature death rate of snails (per day)	0.005–0.033	Anderson and May (1991), Liang et al. (2002)
μ_m	Death rate of mice induced by infection (per day)	0.0005–0.005	Estimated
μ_s	Death rate of snails induced by infection (per day)	0.01–0.55	Guo (1991), Liang et al. (2002)

(ii) Saddle-node bifurcation. We fix $K = 160$ and consider d_m as a parameter which varies from 0 to 0.02. One can find that the stable periodic solution disappears from the supercritical Hopf bifurcation. The number of endemic equilibria changes from $1 \to 2 \to 3 \to 2 \to 1 \to 0$ via two saddle-node bifurcations and a transcritical bifurcation as shown in Fig. 3b.
(iii) Hopf and degenerate Hopf bifurcation. We have observed the Hopf bifurcation in cases *(i)* and *(ii)*. If we fix the parameter $K = 2600$ and change d_m, then from Fig. 3c, we can see a family of stable periodic solutions and a family of unstable periodic solutions when $d_m \in (0.011, 0.012)$. Moreover, we can find the multiple limit cycles region between one Hopf curve and the semi-stable limit cycle curve when $K > 1651.77$ as indicated in Fig. 4. The intersection of Hopf curve and semi-stable limit cycle curve is the degenerate Hopf bifurcation point.
(iv) Bifurcation diagram. We plot the bifurcation curves in the (K, d_m) plane in Fig. 4, and it is consistent with the diagram in Fig. 2. The transcritical bifurcation curve $\Gamma_{\mathscr{R}_0=1}$ is the threshold condition for the outbreak of the disease in terms K and d_m. The blue curves in Fig. 4 are exactly the same saddle-node curves $SN_{1,2}$ in Fig. 2. From simulations, we can see more sophisticated dynamical behaviors. In Fig. 4, two branches of Hopf bifurcation curves are denoted with red lines. We can observe that one branch of Hopf curves is tangent to the saddle-node curve SN_1 indicating the occurrence of the Zero-Hopf bifurcation. We can also find that the system presents the degenerate Hopf bifurcation, while K is large as we mentioned in case *(iii)*.

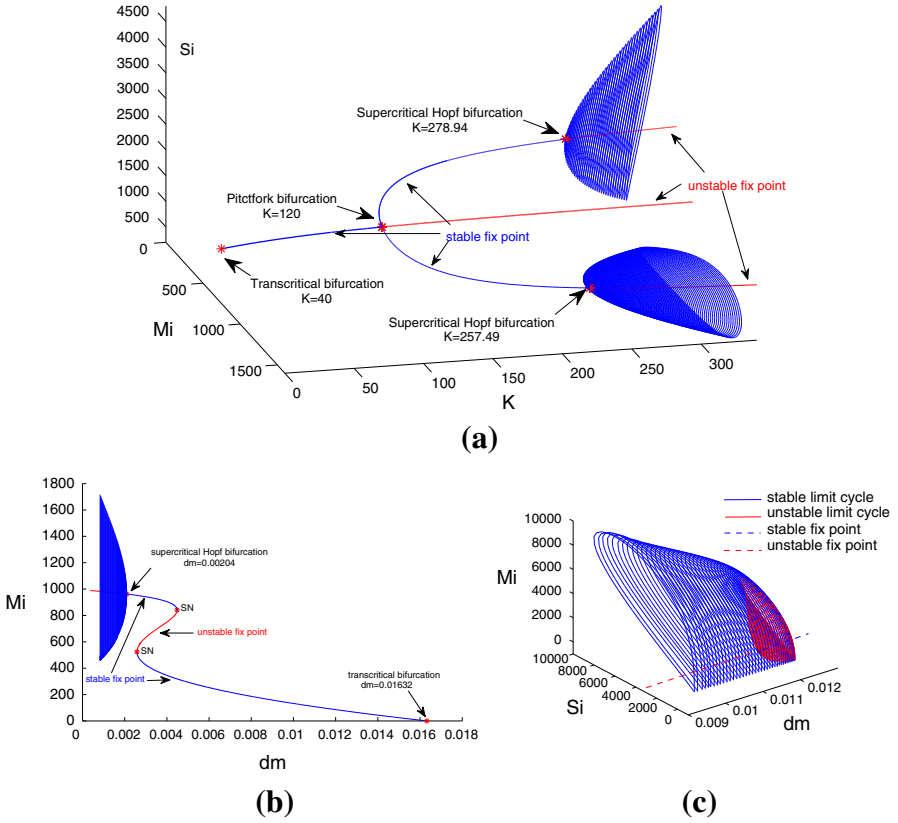

Fig. 3 **a** Pitchfork bifurcation and Hopf bifurcation diagram considering K as a parameter with $d_{\mathrm{m}} = 0.004$. **b** Saddle-node bifurcation and Hopf bifurcation diagram considering d_{m} as a parameter with $K = 160$. **c** Two limit cycles, one stable and the other unstable, bifurcate from the degenerate Hopf bifurcation with $K = 2600$ and $d_{\mathrm{m}} \in (0.11, 0.12)$ (Color figure online)

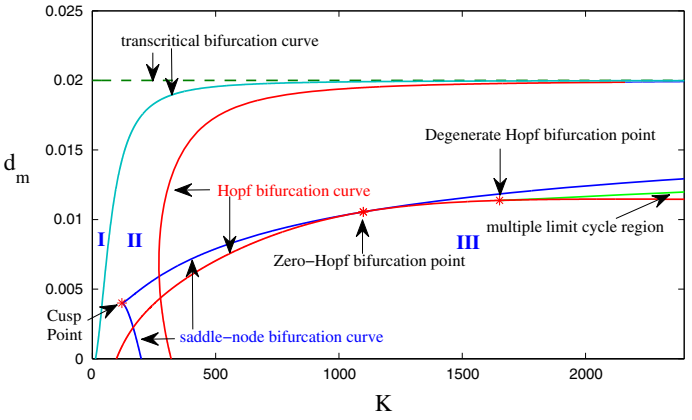

Fig. 4 Bifurcation diagram considering K and d_{m} as parameters (Color figure online)

5 Conclusion and Discussion

Successful interventions in the transmission of schistosomiasis require a better understanding of the influences of the biological and ecological factors. These factors and their interactions can be represented by the parameters in model (1). In this paper, we formulate and analyze a system of ODE model incorporating the impact of the growing islets on the *S. japonica* in the Yangtze River. The center manifold and normal form of the cusp bifurcation of codimension 2 are derived to obtain the existence and stability of the multiple endemic equilibria in the high-dimensional phase space. The bifurcation analysis is carried out to study the influence of the environment, especially the spatial carrying capacity. We give the threshold condition for the outbreak of the disease in terms of the land size. Several kinds of bifurcations are found theoretically and numerically, from which we expand the horizon on the mechanism of schistosomiasis transmission.

Due to the significance of $\mathscr{R}_0$ in epidemiology, it is meaningful to plot the bifurcation curves in the $(\mathscr{R}_0, M_i)$ plane by changing K or d_{m} and fixing the other parameters. We list some typical bifurcation diagrams $(a) - (d)$ in Fig. 5, which agree with Figs. 2, 4.

According to the analyses and simulations in Sects. 3 and 4, it is a challenge to predict, control, and eliminate this disease due to the expansion of islets. The larger the islet becomes, the more complicated the mechanism of the disease transmission will be. Nevertheless, from the formula of $\mathscr{R}_0$, Proposition 3.3, and Fig. 5, we can develop two control strategies as follows:

(1) Use pesticides to kill miracidia, larval, and introduce the predators of snails and mice to decrease the number of these two hosts.
(2) Separate the islet into several small isolated parts by trenches and fences to cut off the movement of mice and snails among these small partitions, and the area of each isolated part is smaller than K_c.

System (1) undergoes several types of bifurcations when $K > K_c$. Biologically speaking, it means different parameters and initial conditions will result in different epidemic levels. The cusp bifurcation of codimension 2 is found, which suggests that the disease can prevail in several different scales. We also observe that the Hopf bifurcation occurs in the model. The existence of Hopf bifurcation indicates the periodic phenomena. Therefore, the recurrence of the schistosomiasis is possible when the initial infection density is in some certain ranges.

The expanding islet provides an advantageous condition for the disease transmission. When the islet reaches a critical size K_{c}, the transmission of the schistosomiasis between the mice *R. norvegicus* and the snails *O. hupensis* will persist, which agrees with the history of the occurrence of schistosomiasis disease in Qian and Zimu islets as shown in Fig. 1. The prevalence of the disease on these islets serves as a possible source of schistosomiasis in the Yangtze valley. Although the disease has been controlled or eradicated, it can still outbreak due to the water flow carrying the schistosome and snails from these endemic islets to the lower reaches of the Yangtze River. A typical example is that the re-emergence of schistosomiasis along the Yangtze River

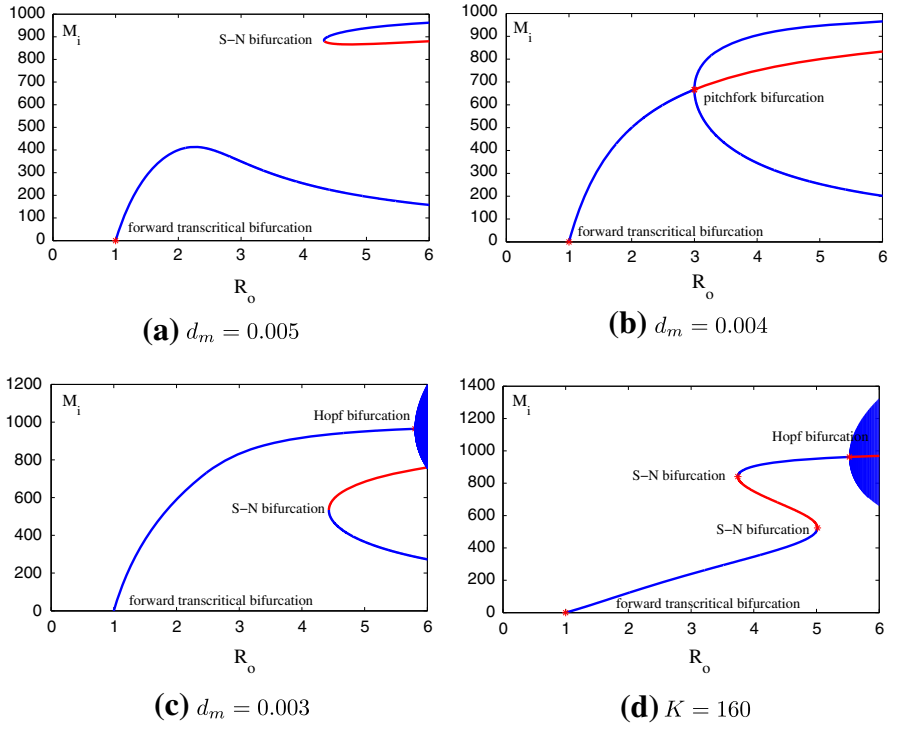

Fig. 5 Some typical bifurcation diagrams in the $(\mathscr{R}_0, M_i)$ plane considering K as a parameter in $(a-c)$ and d_{m} as a parameter in (d). The *blue curves* represent the stable fix points or limit cycles, and *red curves* represent the unstable fix points. In fact, all stable fix points in case $(a-d)$ lose their stability via Hopf bifurcation when $\mathscr{R}_0$ is sufficiently large (Color figure online)

was closely associated with flooding events occurred in 1998, which resulted in schistosome and snails diffusion (Zhao et al. 2005; Zhou et al. 2002, 2005).

Based on the life cycle of schistosomiasis transmission and the cross-infection between the definitive hosts *R. norvegicus* and the intermediate hosts *O. hupensis*, we formulate the model (1), which captures the special feature of schistosomiasis disease. This model is formulated specifically for the schistosomiasis; however, it may be applicable for the other parasitic diseases, which share the common features with schistosomiasis transmission. For example, intermediate hosts and definitive hosts are involved during the transmission of these parasitic diseases, and they can infect each other.

In this paper, we only took into account the influence of the expansion of the islet on the schistosomiasis disease. There are many other natural factors, such as vegetation, soil types, moisture of earth surface, etc., which may contribute to the transmission of *S. japonica* as well. We have also ignored some integrated factors, such as the diffusion of mice and snails, the delay in the disease transmission as well as the possible climate change on the transmission in our study. More insights may be obtained if these factors are included which we leave for future studies.

Acknowledgments This research was supported by NSERC and ERA, an Early Researcher Award of Ministry of Research and Innovation of Ontario, Canada and NSFC-11171267 of China.

References

Anderson RM, May RM (1991) Infectious diseases of humans: dynamics and control. Oxford University Press, New York

Carr L (1981) Applications of centre manifold theory. Springer, New York-Berlin

Castillo-Chavez C, Feng Z, Xu D (2008) A schistosomiasis model with mating structure and time delay. Math Biosci 211:333–341

Chow S-N, Li C, Wang D (1994) Normal forms and bifurcation of planar vector fields. Cambridge University Press, Cambridge

Feng Z, Li C-C, Milner FA (2002) Schistosomiasis models with density dependence and age of infection in snail dynamics. Math Biosci 177/178:271–286

Feng Z, Li C-C, Milner FA (2005) Schistosomiasis models with two migrating human groups. Math Comput Model 41:1213–1230

Hassard BD, Kazarinoff ND, Wan Y-H (1981) Theory and applications of Hopf bifurcation. Cambridge University Press, Cambridge-New York

Gryseels B, Polman Katja, Jan Clerinx, Kestens Luc (2006) Human schistosomiasis. Lancet 368:1106–1118

Guo Y (1991) Snail biology, schistosome biology, prevention and cure of schistosomiasis. People Health Press, Beijing

Liang S, Maszle D, Spear RC (2002) A quantitative framework for a multi-group model of *Schistosomiasis japonicum* transmission dynamics and control in Sichuan, China. Acta Trop 82:263–277

Liang S et al (2007) Environmental effects on parasitic disease transmission exemplified by schistosomiasis in western China. PNAS 104:7110–7115

Kuznetsov Yuri A (1998) Elements of applied bifurcation theory. Springer, New York

MacDonald G (1965) The dynamics of helminth infections with spatial reference to schistosomes. Trans R Soc Trop Med Hyg 59:489–506

Nåsell I, Hirsch WM (1973) The transmission dynamics of schistosomiasis. Commun Pure Appl Math 26:395–453

Poggensee G, Feldmeier H (2001) Female genital schistosomiasis: facts and hypotheses. Acta Trop 79:193–210

Poggensee G, Feldmeier H, Krantz I (1999) Schistosomiasis of the female genital tract: public health aspects. Parasitol Today 15:378–381

Spear RC, Hubbard A, Liang S, Seto E (2002) Disease transmission models for public health decision making: toward an approach for designing intervention strategies for Schistosomiasis japonica. Environ Health Perspect 110:907–915

van den Driessche P, Watmough J (2002) Reproduction numbers and sub-threshold endemic equilibria for compartmental models of disease transmission. Math Biosci 180:29–48

Wu J, Liu N, Zuo S (1987) The qualitative analysis of model of the transmission dynamics of Japanese schistosomiasis. Appl Math A 2:352–362

Wu J, Feng Z (2002) Mathematical models for schistosomiasis with delays and multiple definitive host, mathematical approaches for emerging and reemerging infectious disease: models, methods, and theory (Minneapolis, MN, 1999), 215–229, IMA Vol. Math Appl, 126, Springer, New York

Xu G, Tian J, Chen G, Yang H, Qiu L, Hu H, Xie C, Zhou W, Yin W, Zhao Y, Cai G, Pang H, Wu W (1999) Observation of natural focal disease of schistosomiasis in *Rattus norvegicus* in Nanjing. J Pract Parasitol 7:4–6 (in Chinese)

Zhang P, Feng Z, Milner FA (2007) A schistosomiasis model with an age-structure in human hosts and its application to treatment strategies. Math Biosci 205:83–107

Zhao G, Zhao Q, Jiang Q, Chen X, Wang L, Yuan H (2005) Surveillance for *Schistosomiasis japonica* in China from 2000 to 2003. Acta Trop 96:288–295

Zhao R, Milner FA (2008) A mathematical model of *Schistosoma mansoni* in *Biomphalaria glabrata* with control strategies. Bull Math Biol 70:1886–1905

Zhou X (2005) Science on oncomelania snail. Science Press, Beijing

Zhou X, Lin D, Yang H, Chen H, Sun L, Yang G, Hong Q, Brown L, Malone J (2002) Use of Landsat TM satellite surveillance data to measure the impact of the 1998 flood on snail intermediate host dispersal in the lower Yangtze River basin. Acta Trop 82:199–205

Zhou X, Wang L, Chen M, Wu X, Jiang Q, Chen X, Zheng J, Jury U (2005) The public health significance and control of schistosomiasis in China-then and now. Acta Trop 96:96–105